Appl. Phys. B 92, 305–311 (2008)
DOI: 10.1007/s00340-008-3047-x

Applied Physics B
Lasers and Optics

G. WYSOCKI[1,✉]
R. LEWICKI[2]
R.F. CURL[2]
F.K. TITTEL[2]
L. DIEHL[3]
F. CAPASSO[3]
M. TROCCOLI[3]
G. HOFLER[4]
D. BOUR[4]
S. CORZINE[4]
R. MAULINI[5]
M. GIOVANNINI[5]
J. FAIST[5,6]

Widely tunable mode-hop free external cavity quantum cascade lasers for high resolution spectroscopy and chemical sensing

[1] Electrical Engineering Department, Princeton University, Engineering Quadrangle, Olden Street, Princeton, NJ 08544, USA
[2] Rice Quantum Institute, Rice University, 6100 Main St., Houston, TX 77005, USA
[3] School of Engineering and Applied Sciences, Harvard University, 9 Oxford Street, Cambridge, MA 02138, USA
[4] Agilent Laboratories, 3500 Deer Creek Road, Palo Alto, CA 94304, USA
[5] Institute of Physics, University of Neuchâtel, 1 A.-L. Breguet, 2000 Neuchâtel, Switzerland
[6] ETH Zurich, Wolfgang-Pauli Str. 16, 8093 Zurich, Switzerland

Received: 15 January 2008/Revised version: 17 April 2008
Published online: 31 May 2008 •

ABSTRACT Recent progress in the development of room temperature, continuous wave, widely tunable, mode-hop-free mid-infrared external cavity quantum cascade laser (EC-QCL) spectroscopic sources is reported. A single mode tuning range of 155 cm^{-1} ($\sim 8\%$ of the center wavelength) with a maximum power of 11.1 mW and 182 cm^{-1} ($\sim 15\%$ of the center wavelength) with a maximum power of 50 mW was obtained for 5.3 and 8.4 μm EC-QCLs respectively. This technology is particularly suitable for high resolution spectroscopic applications, multi species trace-gas detection and spectroscopic measurements of broadband absorbers. Several examples of spectroscopic measurements performed using EC-QCL based spectrometers are demonstrated.

PACS 42.55.Px; 42.60.-v; 42.62.Fi; 07.07.Df

1 Introduction

The invention of quantum cascade lasers (QCLs) [1], has led to a significant progress in mid-IR spectroscopy and its applications to trace gas sensing. High power (50–500 mW), room temperature operation with thermoelectric cooling (TEC), and continuously improving wall plug efficiency of continuous wave (cw) and pulsed QCL designs [2–6], make them suitable field deployable sources for most demanding real-world chemical sensing applications. For accurate spectroscopic analysis [7, 8], both single transverse and longitudinal mode operation for QCLs are required. The latter can be achieved either by embedding within the QCL active region a periodic structure that provides distributed feedback (DFB) for a single longitudinal laser mode at a precisely selected wavelength [6, 9], or by using an external cavity configuration (EC) [10–14].

The wavelength tunability of DFB QCLs relies on thermal tuning of the refractive index, which limits the frequency coverage to ~ 10–$20\,cm^{-1}$ when slow temperature tuning is applied or to ~ 2–$3\,cm^{-1}$ when fast Joule heating by an injection current is used. Thermal tuning strongly affects the QCL threshold resulting in a decrease of the output power at higher chip temperatures. Thus DFB-QCLs are typically designed to target absorption lines of one specific molecule with narrow, well resolved ro-vibrational absorption lines. Substantially low fabrication yield of DFB-QCLs operating at precisely selected wavelengths has limited the availability of commercial QCLs to wavelengths that correspond to absorption by molecules of widespread interest. The application of an EC configuration allows selection of the QCL wavelength anywhere within the available QCL spectral gain without changing the chip temperature, thus significantly increasing the laser spectral coverage and allowing much more efficient utilization of the available QCL spectral gain.

This is especially important for the QCL gain media designed to have intrinsically broader gain profiles. This includes bound-to-continuum QCLs in which the lower state of the laser transition is a relatively broad continuum [15, 16] or heterogeneous QCL structures with ultra-broad optical gain. The latter design that consists of multiple active regions that support laser transitions at different wavelength was first demonstrated by Gmachl et al. [17]. Recently frequency tunability from 961 to 1220 cm^{-1} ($\sim 24\%$ of the center wavelength) of a pulsed QCL was achieved using a heterogeneous gain medium with a two-wavelength (8.4 and 9.6 μm) active region in a Littrow type EC-QCL configuration [12].

Although the wavelength tuning speeds available with an EC configuration are slower than for DFB-QCLs, the EC-QCLs have already proven to be interesting alternative spectroscopic sources that can enable new applications such as agile detection of multiple gases including those with broad absorption bands [10, 18, 19]. At present the alternative means for achieving broad spectral coverage is multiple DFB QCL arrays with a varying DFB grating period [6, 20].

In this work we report the development of a cw, TEC cooled, EC-QCL technology with specific emphasis on applications that require broadband, high resolution spectroscopy. Two EC-QCL sources based on the same EC architecture but employing two different gain media have been investigated.

✉ Fax: +1-609-258-2158, E-mail: gwysocki@princeton.edu

The QCL chips utilized were fabricated using significantly different technologies:

1) the QCL operating at 5.3 μm with a bound-to-continuum design of the active region grown used a molecular beam epitaxy (MBE) process and was fabricated with a standard ridge waveguide structure, and
2) the QCL operating at 8.4 μm employed a double-phonon resonance design of the active region which was grown using metal organic vapor-phase epitaxy (MOVPE) process and fabricated as a buried heterostructure.

Some important aspects of the two technologies will be discussed below, and the performance and the spectroscopic applications of the EC-QCL technology will be demonstrated.

2 EC-QCL configuration

The EC-QCL system is an improved miniaturized version of the source reported in [10]. The optical configuration of the Littrow type EC-QCL is shown schematically in Fig. 1a. The overall size of the system is ∼ 9 in × 6 in × 6 in (∼ 23 cm × 15 cm × 15 cm). It consists of a QCL housing and an electrically controlled external cavity positioning system (see Fig. 1b). The present system has proved to be a convenient research tool, which allows investigation and testing of the EC-QCL components using off-the-shelf optics (e.g. collimating lenses, diffraction gratings and QCL gain chips). The laser housing is equipped with an integrated TEC cooling system capable of operating the QCL at temperatures as low as −40 °C with optional external chilled water cooling. The housing is vacuum-tight and incorporates a manual 3D lens positioning system that accepts collimating optics up to 1 inch in diameter. As in the previous system the EC arrangement consists of three main elements: the QCL chip, a beam collimating lens, and a diffraction grating. The zeroth order reflection from the grating is reflected from the mirror, M mounted together with the grating on the same rotary platform providing the output laser beam. This configuration provides an output laser beam fixed in location and direction during the wavelength tuning process. This fixed beam is achieved by precise alignment of the grating and the mirror M in such a way that the planes collinear with both reflecting surfaces intersect exactly at the rotation axis of the rotary platform. The previous system could only provide a fixed direction of the laser beam, but the beam was subject to parallel walk-off while the laser wavelength was tuned. The piezo-activated mode-tracking system that provides independent control of the EC length and diffraction grating angle for mode-hop free tuning was adopted from the previous system [10]. The flexibility of this EC architecture makes it compatible with any QCL gain chip at any mid-infrared wavelength without changing the EC configuration. The performance of the new system was demonstrated with two cw, TEC, Fabry–Pérot QCL gain chips operating at ∼ 5.3 and 8.4 μm, respectively.

2.1 *EC-QCL operating at 5.3 μm*

2.1.1 Technical details. The gain chip with a ridge waveguide width of 12 μm and length of 2.25 mm was used to construct an EC QCL operating at 5.3 μm. The EC feedback was obtained using a first order diffraction from the Littrow type diffraction grating with 150 grooves/mm, ∼ 93% reflectivity and blaze angle optimized for λ = 5.4 μm (Optometrics, model: ML401). The QCL chip was fabricated as a standard ridge waveguide structure and an active region based on bound-to-continuum design [21]. Since in the bound-to-continuum scheme the lower state of the laser transition is essentially a broad continuum the QCLs based on this technology exhibit a broadened gain profile. A high-reflection (HR) coating (Al_2O_3/Au 300 nm/100 nm) was deposited on the back facet and an anti-reflection (AR) coating (a multilayer dielectric AR coating [22]) was deposited on the front facet of the chip. Figure 2 shows the LIV curves measured for the QCL chip at −30 °C at different stages of the chip fabrication. The characteristic threshold currents densities for the

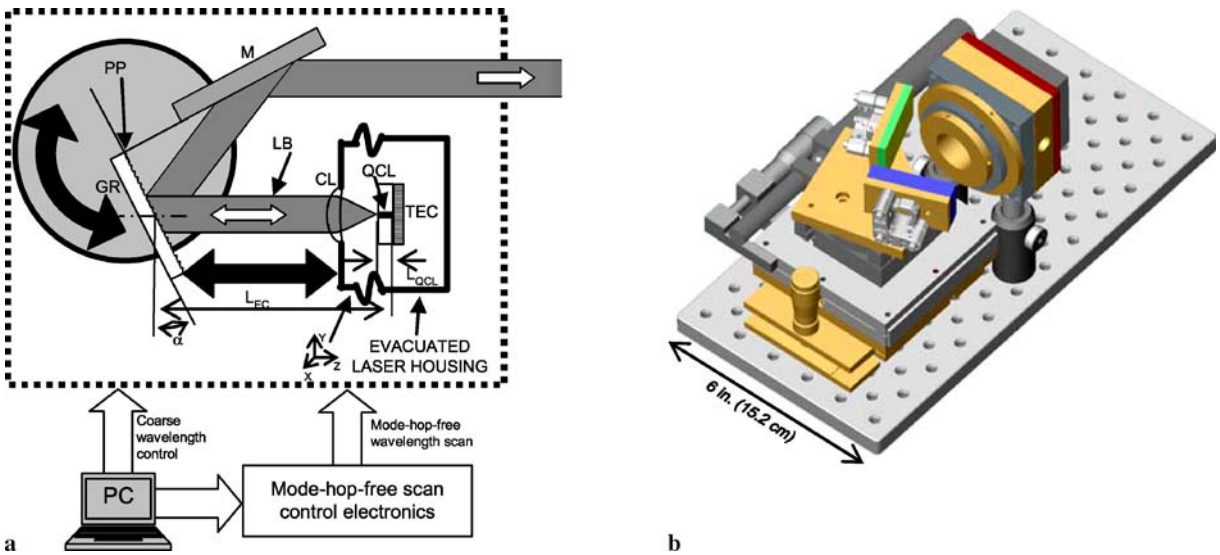

FIGURE 1 (**a**) Schematic diagram of the EC-QCL spectroscopic source configuration (QCL – quantum cascade laser; TEC – thermoelectric cooler; CL – collimating lens; LB – laser beam; GR – diffraction grating; PP – pivot point of the rotational movement; M – mirror mounted on the same platform with GR). (**b**) A 3D model of the EC-QCL source assembly

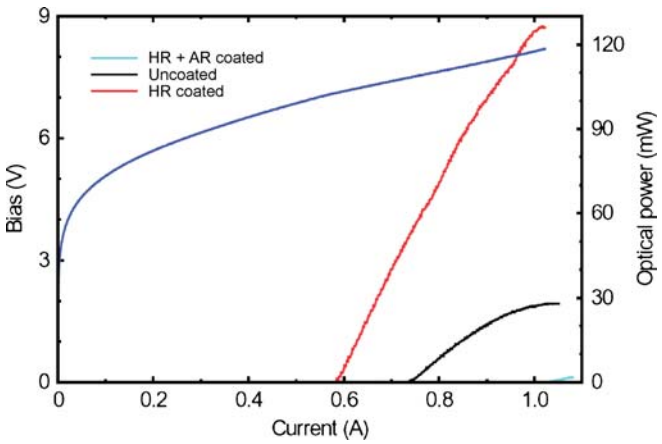

FIGURE 2 LIV curves for the 5.3 μm QCL gain medium operated at −30 °C. The *curves* were measured at different stages of the QCL chip processing

current chip operated at −30 °C are: $J_{\mathrm{th(UC)}} = 2.72\,\mathrm{kA/cm^2}$, $J_{\mathrm{th(HR)}} = 2.15\,\mathrm{kA/cm^2}$, $J_{\mathrm{th(HR+AR)}} = 3.82\,\mathrm{kA/cm^2}$, for an uncoated chip (with facet reflectivity of 27.4%), a HR coated back facet (with reflectivity of 95%), and a HR and AR coated chip respectively. A threshold current of 566 mA measured with EC feedback at the center of the gain curve yielded a threshold current density of $J_{\mathrm{th(EC)}} = 2.1\,\mathrm{kA/cm^2}$. Using the relation between the resonator losses and laser threshold current [23], these current densities allow the waveguide losses to be estimated as $\alpha_{\mathrm{w}} \approx 5.64\,\mathrm{cm^{-1}}$, the total EC optical feedback to be estimated as ∼ 31%, and the calculation of the AR coating reflectance yields ∼ 0.7%. QCL wavelength tuning was evaluated using a 1/8 m monochromator (CVI model: CM110).

Figure 3 shows power normalized spectra recorded for several positions of the diffraction grating within the tuning range of the EC-QCL operated at 950 mA together with the corresponding optical power. This EC-QCL has a maximum tuning range of 155 $\mathrm{cm^{-1}}$ with an output power of up to 11.1 mW at the center of the gain profile.

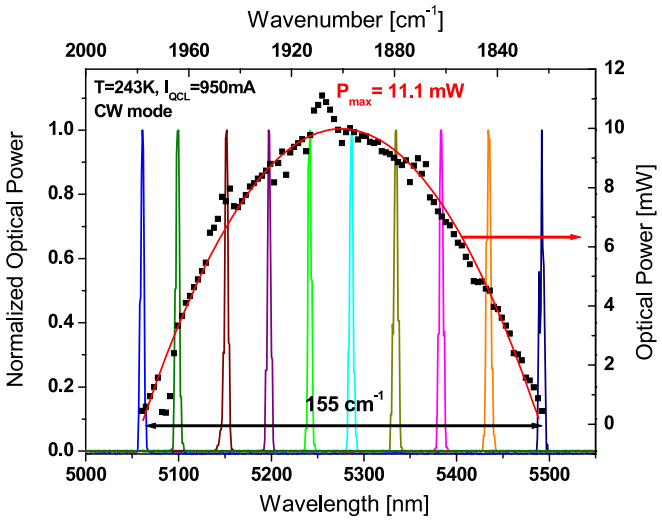

FIGURE 3 Laser frequency tuning range and corresponding optical power of the 5.3 μm EC-QCL operated in cw at 950 mA and −30 °C

Mode-hop-free laser frequency tuning with a spectral resolution of $< 0.001\,\mathrm{cm^{-1}}$ ($<\sim 30$ MHz) is primarily limited by the laser linewidth and can be used for high resolution spectroscopic applications. A mode-hop-free scan can be performed at any available laser wavelength with a maximum frequency scan range of $\sim 2.5\,\mathrm{cm^{-1}}$ limited primarily by the maximum available excursion of the PZT element (90 μm) controlling the EC length. Unlike the previous system [10], in which the available dynamic range of QCL current tuning (between laser threshold and power rollover) was the parameter limiting the maximum mode-hop-free tuning range, in this 5.3 μm EC-QCL the dynamic range of 400 mA (at −30 °C) should allow a mode-hop-free scan of $\sim 4\,\mathrm{cm^{-1}}$ (estimated using the typical FP mode tuning rate of $\sim 0.01\,\mathrm{cm^{-1}/mA}$). This increased tuning range should be achievable either by employing a PZT element with a maximum travel of 150 μm or by a further reduction of the EC length from its current ∼ 7 to ∼ 4.7 cm. Of course at the extremes of the total tuning range, the EC-QCL experiences a reduction of the available laser gain and the mode-hop-free range may become current dynamic range limited.

Maximum scan rates in opto-mechanical systems are usually limited by relatively low frequency mechanical vibration resonances. The EC-QCL system reported in this work consists of commercially available components and the first mechanical resonance frequency of the system associated with cavity length control was found to be at $f_{\mathrm{m}} = \sim 68$ Hz. Sinusoidal signals at frequencies lower than $0.8\,f_{\mathrm{m}}$, should provide optimum operating conditions for EC-QCL wavelength scanning. The electronics used in this work to drive the piezo actuators allows the maximum piezo travel range (providing a $\sim 2.5\,\mathrm{cm^{-1}}$ laser frequency scan) to be achieved with scanning frequencies ≤ 22 Hz.

The transverse mode structure of the laser was also examined. The far field emission pattern of the output laser beam collimated with a 1.89 mm, focal length $f/0.52$ ZnSe aspheric lens (provided for this laser by Daylight Solutions) was imaged with a mid-IR camera (Electrophysics model: PV320LZ). Since the threshold current of the AR coated chip was close to the cw power rollover region the far field measurement of the QCL output without the EC was observed in a pulsed mode just above the lasing threshold. The 5.3 μm QCL with a relatively wide ridge of 12 μm (∼ 38 μm in optical distance, which is equivalent of ∼ 7λ) operates in higher order lateral mode, $\mathrm{TM_{02}}$ as shown in Fig. 4a. When the QCL was placed in an EC configuration and operated cw both the $\mathrm{TM_{01}}$ and $\mathrm{TM_{00}}$ modes were observed with relative intensities strongly dependent on the actual EC alignment. A stable $\mathrm{TM_{00}}$ operation within the entire EC-QCL wavelength tuning range could be achieved after introduction of an additional optical diaphragm inside the laser cavity that restricted the laser operation to a fundamental lateral mode $\mathrm{TM_{00}}$. A far field EC-QCL emission pattern recorded for cw operation at 900 mA is shown in Fig. 4b. The intensity profile of the laser beam is slightly elliptical, but a quasi-Gaussian distribution is observed in both axes as shown in Fig. 4b. The collimating lens results in an output beam diameter of ∼ 4 mm.

Compared to the previous EC-QCL system described in [10] the reduction of the beam diameter by a factor of 5 while maintaining the other parameters, caused a reduction of

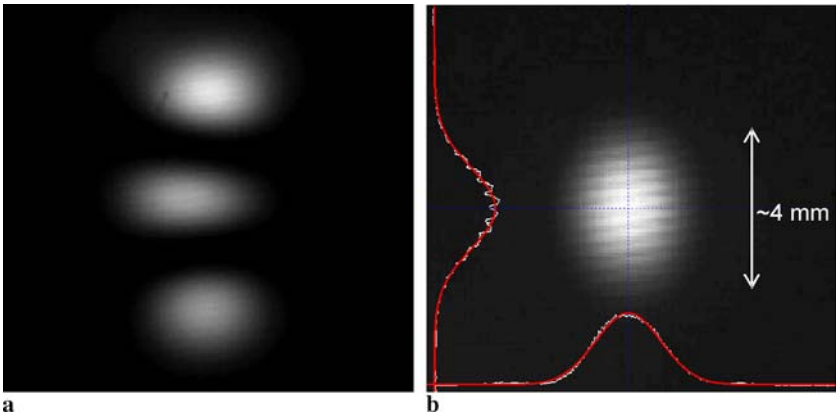

FIGURE 4 (**a**) Laser beam profile recorded for the 5.3 μm QCL FP chip operated in a pulsed mode. (**b**) Laser beam profile measured for the same QCL chip operated cw in EC configuration. The cross-sections along the *dotted lines* are shown with a fit by a Gaussian curve (*red lines*). The same collimating lens was used in (**a**) and (**b**). The interference fringes visible in the images result from some parasitic reflections in the optical system and are not an intrinsic feature of the EC-QCL

the grating resolving power by the same factor. This yields a grating spectral bandwidth of $\sim 3\,\mathrm{cm}^{-1}$. With an EC optical length of ~ 7 cm and QCL optical length of ~ 7 mm, which corresponds to a free spectral range (FSR) of 0.07 and $0.72\,\mathrm{cm}^{-1}$ respectively, ~ 42 longitudinal EC Fabry–Pérot (FP) modes and ~ 4 QCL FP modes are within the grating spectral bandwidth simultaneously. Since the gain section of the EC-QCL is adjacent to one of the resonator mirrors, the EC FP modes located in close spectral proximity to the lasing mode ν_0 occupy nearly the same physical space in the active region and multimode operation caused by spatial hole burning phenomena will not occur. However for the EC modes at frequencies separated by at least the QCL FSR hole burning and thus multimode operation may occur. However in this system despite the large grating bandwidth the cavity losses at frequencies $\leq (\nu_0 - \mathrm{FSR_{QCL}})$ and $\geq (\nu_0 + \mathrm{FSR_{QCL}})$ are sufficiently high to maintain a stable single mode operation at ν_0.

2.1.2 Example spectroscopic applications. Both features, wide tunability and the capability of mode-hop-free tuning of the reported EC-QCL system, have a vital role in spectroscopic applications. Measurement of broad absorption features (of large molecules in the gas phase, liquids, and/or solid samples), as well as simultaneous detection of multiple trace gas species can greatly benefit from the broad tunability offered by EC-QCL lasers. The combination of broadband tuning and high resolution fine tuning in this EC system can alleviate the problem of obtaining a QCL with a wavelength that coincides with the optimum absorption wavelength of a particular trace gas species as mentioned above. At 5.3 μm, nitric oxide (NO) detection and monitoring can be performed. This capability is of great importance for biomedical applications (e.g. for breath analysis), environmental applications (NO is an environmental pollutant) [8], or industrial applications (e.g. combustion process control) [24]. Broad wavelength coverage provides the ability to select a target NO absorption line that is free of spectral interference from other species such as water (H_2O) or carbon dioxide (CO_2) as shown in Fig. 5a, is a critical requirement in the aforementioned applications.

A situation in which target line selection is even more restrictive is the detection of NO using a Faraday rotation spectroscopy [25–27]. As predicted by Ganser et al. [26] the best NO Faraday detection limit should be obtained for the $Q(3/2)$ transition at $1875.8\,\mathrm{cm}^{-1}$, which has the highest magnetic modulation sensitivity. However targeting of this line has not been possible to-date using commercially available DFB QCLs, which are usually optimized to operate either in a *P*- or *R*-branch of the NO fundamental band. As shown in Fig. 5a, the 5.3 μm EC-QCL can cover almost entirely the *P*-, *Q*- and *R*-branches of the NO fundamental absorption band at ~ 5.3 μm, and allows performing the Faraday rotation spectroscopic detection of NO using the most optimum rotational component in the *Q*-branch (see the measured high resolution direct absorption spectrum in Fig. 5b). An example Faraday spectrum of the NO $Q(3/2)$ and $Q(5/2)$ transitions acquired for a 10 ppm of NO in N_2 as a buffer gas within a 42 cm active optical pathlength with a minimum detection limit of ~ 5.5 ppb is shown in Fig. 5c. The performance characteristics of a NO EC-QCL based Faraday rotation spectrometer is currently under investigation and will be reported elsewhere [28].

To demonstrate spectroscopic measurements of broadband absorbing species a quartz enhanced photoacoustic spectrum (QEPAS) [29], of a gas mixture containing 7.2% ethanol and 0.24% H_2O in N_2 as a buffer gas was measured using the 5.3 μm EC-QCL. The results along with reference spectra of ethanol and water vapor are shown in Fig. 6. Coarse wavelength scanning together with 50% duty cycle direct laser current amplitude modulation (with 100% modulation depth) at ~ 32 kHz and QEPAS based on AM detection was used in this measurement [18, 19]. The signal is laser power normalized to eliminate any laser power fluctuations related to mode-hoping (up to 3%) that might occur during a coarse wavelength scan, and to account for an absorption by atmospheric water within an open optical path of the system. Despite a strong QCL chirp during the laser current pulse combined with a grating spectral bandwidth of $3\,\mathrm{cm}^{-1}$, which in this case should reflect the minimum effective resolution of the system, the narrow water lines can still be clearly identified in the measured spectrum. The actual resolution of the system could be estimated to be $\sim 1.2\,\mathrm{cm}^{-1}$ using a full width at half maximum measured for several isolated water lines observed in the spectrum.

QCL frequency chirping can be avoided by using cw operation of the laser and an indirect (external) intensity modulation by means of a beam chopper, an electro-optical modulator or an acousto-optical modulator. However applicability of a mechanical beam chopper for QEPAS requires a rela-

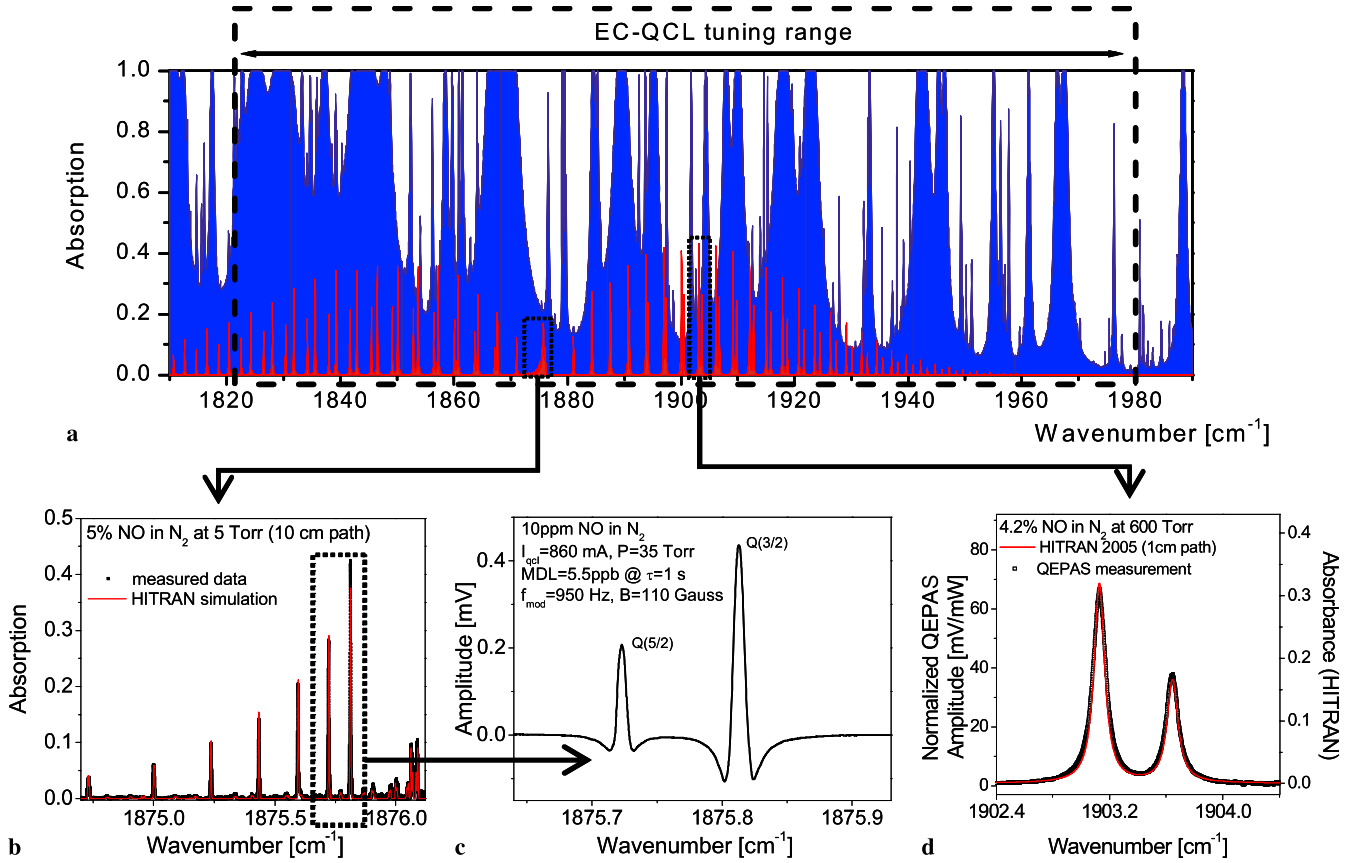

FIGURE 5 (**a**) Simulation of atmospheric absorption (*in blue*) over a 286 m path within the 5.3 μm EC-QCL tuning range (H_2O mixing ratio = 0.6%, CO_2 mixing ratio = 380 ppm, $P = 760$ Torr, $T = 276$ K). For reference an absorption spectrum of 1 ppm NO at the same working condition is plotted (*in red*). *Lower panels* demonstrate a mode-hop-free spectra of NO acquired as: (**b**) a direct absorption spectrum of the NO Q-branch recorded at scan rate of 10 Hz for 5% NO in N_2 at reduced pressure and with 10 cm optical path length (*red line* shows a well matching HITRAN spectrum simulated for the same conditions), (**c**) a Faraday rotation spectrum of NO $Q(3/2)$ and $Q(5/2)$ transitions at ∼ 1875.8 cm^{-1} for 10 ppm NO in N_2 mixture at 35 Torr and with 42 cm active optical pathlength (the minimum detection limit estimated as MDL = 5.5 ppb), and (**d**) a QEPAS spectrum recorded for 4.2% NO in N_2 at ∼ 1903 cm^{-1}, pressure of 600 Torr and with 1 cm optical pathlength (the strongest transition in the fundamental NO R-branch)

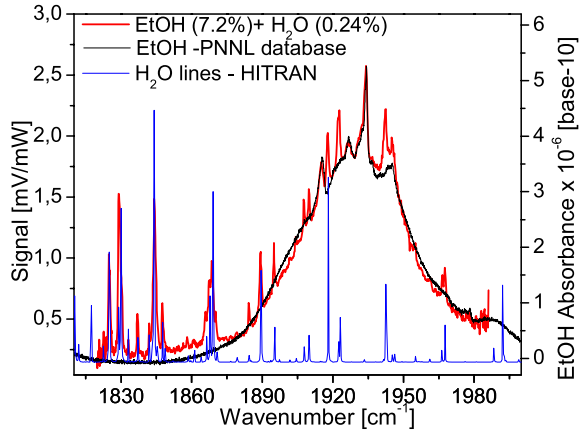

FIGURE 6 Photoacoustic spectrum of a gas mixture containing 7.2% ethanol and 0.24% H_2O in N_2 as a buffer gas measured at atmospheric pressure using a 5.3 μm EC-QCL (*red line*). Absorption spectra of ethanol (*black line*) and water vapor (*blue line*) obtained from the PNNL database and the HITRAN database respectively are plotted for reference

tively high chopping frequency, which is not easy to realize in practice. In our case the 32 kHz amplitude modulation can be realized up to ∼ 80% modulation depth using a quartz tuning fork similar to the one used in the QEPAS based gas sensor as a chopper. A mode-hop-free spectrum of 4.2% NO in N_2 at 1903 cm^{-1} in Fig. 5d clearly demonstrates the high resolution capability of an EC-QCL based photoacoustic spectrometer. It should be noted that for the spectra acquired using techniques that employ a phase sensitive lock-in detection (in our case both Faraday rotation spectroscopy and QEPAS) the relatively slow wavelength scanning rate of the EC-QCL is not a limiting parameter. The applied lock-in time constant determines the time necessary to acquire signal for each spectral point within the scan.

2.2 *High power EC-QCL operating at 8.4 μm*

2.2.1 Technical details. The EC-QCL operating at 8.4 μm was constructed using a new MOCVD grown buried heterostructure Fabry–Pérot QCL gain chip operating at 8.4 μm [5] (with a waveguide width of 5 μm, and length of 3 mm) in the same EC-QCL architecture as that used for 5.3 μm. For better performance a grating with 135 grooves/mm and a grazing angle optimized for the longer wavelengths was used (nominal blaze angle optimized for $\lambda = 10.6$ μm and efficiency > 90% between 6.5 and 13.5 μm). For beam collimation an AR coated (3–12 μm) $f/0.6$ germanium aspheric lens with 24 mm-diameter (Optical Solu-

tions, model: 4682) was incorporated, which provided an output beam with a diameter of ∼ 20 mm. Similar to the 5.3 μm QCL chip a high-reflection (HR) coating (Al_2O_3/Au 300 nm/100 nm) was deposited on the back facet and an AR coating (the same multilayer dielectric AR coating [22] could also be used in this wavelength region with appropriate design of the layer thicknesses) was deposited on the front facet of the 8.4 μm QCL chip. Figure 7 shows the LIV curves measured for the QCL chip at −30 °C at different stages of the chip fabrication. Using the characteristic threshold currents densities for the QCL operated at −30 °C: $J_{th(UC)} = 1.37\,kA/cm^2$, $J_{th(HR)} = 1.13\,kA/cm^2$, $J_{th(HR+AR)} = 2.33\,kA/cm^2$ and $J_{th(EC)} = 1.03\,kA/cm^2$, the uncoated facet reflectivity of 27.4% and the HR coated facet reflectivity of 95%, the estimates of the waveguide losses, the total EC optical feedback, and the AR coating reflectance yielded: $\alpha_w \approx 7.8\,cm^{-1}$, ∼ 46.7%, and ∼ 0.046% respectively. We attribute such an excellent AR coating quality to the much higher uniformity of the deposited coating over the area of the guided mode field at the facet of a buried heterostructure QCL waveguide. In the ridge waveguide structure the mode field is adjacent to the side wall edges, which may introduce AR coating thickness variations, thus decreasing the coating quality.

The combination of a high performance QCL chip, a high quality AR coating and strong EC feedback (due to a combination of a very fast aspheric lens and optimized diffraction grating) resulted in single mode laser frequency tuning of 182 cm^{-1}, which is ∼ 15% of the center wavelength. To our best knowledge this is the best result reported to-date for a cw EC system employing a QCL chip with a standard (double-phonon resonance) design of the active region. If the same processing steps were applied for a QCL with a bound-to-continuum transition, an even broader tuning range might be possible. Figure 8 depicts spectral measurements of the laser output radiation for several different diffraction grating angles recorded together with a corresponding laser power measured at a driving QCL current of 420 mA. The maximum cw power of ∼ 50 mW was measured for the 8.4 μm EC-QCL operated at a heatsink temperature of −30 °C and a driving current of ∼ 750 mA (see Fig. 7). The laser exhibited a stable fundamental TM_{00} lateral mode operation and did not require an additional intracavity optical diaphragm for transverse mode restriction.

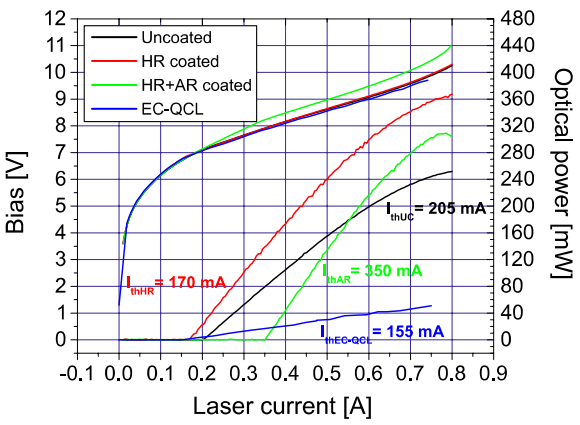

FIGURE 7 LIV curves for the 8.4 μm MOCVD grown QCL gain medium operated at −30 °C. The *curves* were measured at different stages of the chip processing and after its incorporation into the EC-QCL configuration

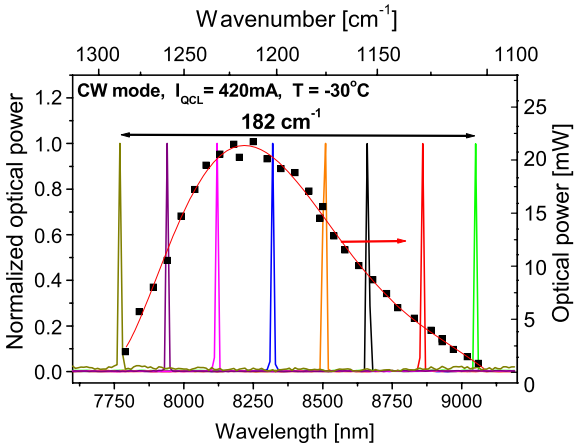

FIGURE 8 Laser frequency tuning range and corresponding optical power of the 8.4 μm EC-QCL operated in cw at 420 mA and −30 °C

The 8.4 μm EC-QCL can also perform mode-hop-free tuning using similar opto-mechanical and PZT components as for the above described 5.3 μm laser system. The optical EC length in this system is also ∼ 7 cm including the QCL chip optical length of ∼ 1 cm, which corresponds to EC FSR of 0.07 cm^{-1} and FP QCL FSR of 0.5 cm^{-1} respectively. The maximum mode-hop-free tuning, which in this case is also limited by the 100 μm PZT range, can be performed over up to ∼ 1.7 cm^{-1} with a spectral resolution of < 0.001 cm^{-1} (∼ 30 MHz).

2.2.2 Example spectroscopic applications. The 8.4 μm EC-QCL with a tuning range between 7.77 and 9.05 μm (spanning over 1.28 μm) and a maximum cw output power of 50 mW represent an excellent spectroscopic source for a number of laser spectroscopic applications. Some specific applications such as remote sensing or photoacoustic spectroscopy can directly benefit from the high output power levels. Several molecules possess strong absorption bands within the tuning range of the laser. Figure 9a shows absorption line strengths for several environmentally important molecules obtained from the HITRAN 2004 database that are accessible with this EC-QCL source. An absorption spectrum of a pure nitrous oxide (N_2O) sample at reduced pressure of 5 Torr and with 5 cm optical path was acquired using a mode-hop-free scanned EC-QCL. Figure 9b shows an excellent agreement between the measured and database simulated spectrum of Doppler broadened N_2O lines confirming the high resolution capability of the reported system.

An earlier version of the 8.4 μm EC-QCL was also extensively tested as a spectroscopic source in a photoacoustic spectrometer (QEPAS) used for detection and quantification of broadband absorbers. The experimental results including concentration measurements (at ppb levels) of Freon 125A (C_2HF_5) and acetone as well as the quantification of the molecular concentrations in a mixture of both compounds are reported in [19]. The performance of this EC-QCL was further optimized and is also reported in the manuscript.

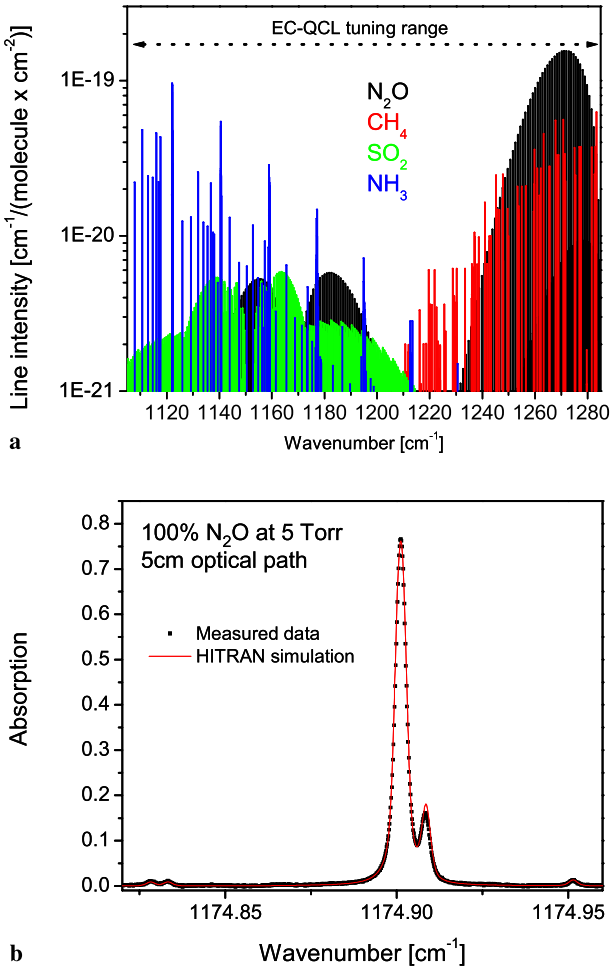

FIGURE 9 (**a**) HITRAN 2000 based simulation of absorption line strength for several molecules including: nitrous oxide (N_2O), methane (CH_4), sulfur dioxide (SO_2), and ammonia (NH_3) within the tuning range of the 8.4 μm EC-QCL laser. (**b**) N_2O spectrum at ∼ 1174.9 cm^{-1} recorded using a mode-hop-free scan (single spectrum recorded at 22 Hz scan rate) of the EC-QCL (*black dots*) together with HITRAN simulated spectrum (*red line*)

3 Conclusions

The technical details and spectroscopic capabilities of the new EC-QCL system have been described. The reported EC architecture allows the use of QCL chips at any wavelength within the mid-IR molecular fingerprint region (3–20 μm), as was demonstrated using two QCLs at 5.3 and 8.4 μm respectively. The 5.3 μm EC-QCL is an ideal source for NO measurements since it covers almost the entire spectral region of the *P*-, *Q*- and *R*-branches of the fundamental NO vibration. This allows a convenient access to less common absorption line targets within the NO spectrum. By targeting a specific line in the *Q*-branch, ultra sensitive Faraday rotation measurements of NO could be performed. The 8.4 μm EC-QCL, capable of high resolution mode-hop free frequency tuning with a tunability of up to 15% of the central wavelength and an output power of up to 50 mW at a TEC achievable QCL temperature of −30 °C, shows the excellent potential of the EC-QCL technology for compact, high resolution broadband laser based mid-IR spectrometers. A few examples of molecular spectroscopic applications including direct absorption spectroscopy, photoacoustic spectroscopy, and Faraday rotation spectroscopy demonstrate the flexibility of the technology developed and the benefits of both the wide tunability and high resolution of the EC-QCL based systems.

ACKNOWLEDGEMENTS The authors acknowledge financial support from the MIRTHE NSF ERC, a subaward of a DoE STTR Grant from Aerodyne Research, and the Robert Welch Foundation. The Harvard group acknowledges partial financial support of the development of the gain medium at 8.4 μm from the U.S. Army Research Office under Grant No. W911NF-04-1-0253 and also support from the Center for Nanoscale Systems (CNS) at Harvard University. Harvard-CNS is a member of the National Nanotechnology Infrastructure Network (NNIN). The development of the gain medium at 5.3 μm and AR-coating technology by ETHZ/University of Neuchâtel team was supported by the NCCR-Quantum Photonics.

REFERENCES

1 J. Faist, F. Capasso, D.L. Sivco, C. Sirtori, A.A. Hutchinson, A.Y. Cho, Science **264**, 4 (1994)
2 J. Faist, Appl. Phys. Lett. **90**, 253 512 (2007)
3 J.S. Yu, A. Evans, S. Slivken, S.R. Darvish, M. Razeghi, IEEE Photon. Technol. Lett. **17**, 1154 (2005)
4 A. Evans, S.R. Darvish, S. Slivken, J. Nguyen, Y. Bai, M. Razeghi, Appl. Phys. Lett. **91**, 071 101 (2007)
5 L. Diehl, D. Bour, S. Corzine, J. Zhu, G. Hofler, M. Loncar, M. Troccoli, F. Capasso, Appl. Phys. Lett. **88**, 201 115 (2006)
6 A. Wittmann, M. Giovannini, J. Faist, L. Hvozdara, S. Blaser, D. Hofstetter, E. Gini, Appl. Phys. Lett. **89**, 141 116 (2006)
7 D.D. Nelson, B. McManus, S. Urbanski, S. Herndon, M.S. Zahniser, Spectrochim. Acta A **60**, 3325 (2004)
8 B.W.M. Moeskops, S.M. Cristescu, F.J.M. Harren, Opt. Lett. **31**, 823 (2006)
9 T. Aellen, S. Blaser, M. Beck, D. Hofstetter, J. Faist, E. Gini, Appl. Phys. Lett. **83**, 1929 (2003)
10 G. Wysocki, R.F. Curl, F.K. Tittel, R. Maulini, J.M. Bulliard, J. Faist, Appl. Phys. B **81**, 769 (2005)
11 C. Peng, G. Luo, H.Q. Le, Appl. Opt. **42**, 4877 (2003)
12 R. Maulini, A. Mohan, M. Giovannini, J. Faist, E. Gini, Appl. Phys. Lett. **88**, 201 113 (2006)
13 M.J. Weida, D. Arnone, T. Day, Laser Focus World **42**, 2 (2006)
14 A. Mohan, A. Wittmann, A. Hugi, S. Blaser, M. Giovannini, J. Faist, Opt. Lett. **32**, 2792 (2007)
15 J. Faist, M. Beck, T. Aellen, E. Gini, Appl. Phys. Lett. **78**, 147 (2001)
16 A. Wittmann, T. Gresch, E. Gini, L. Hvozdara, N. Hoyler, M. Giovannini, J. Faist, IEEE J. Quantum Electron. **QE-44**, 36 (2008)
17 C. Gmachl, D.L. Sivco, R. Colombelli, F. Capasso, A.Y. Cho, Nature **415**, 5 (2002)
18 M.C. Phillips, T.L. Myers, M.D. Wojcik, B.D. Cannon, Opt. Lett. **32**, 1177 (2007)
19 R. Lewicki, G. Wysocki, A.A. Kosterev, F.K. Tittel, Opt. Express **15**, 7357 (2007)
20 B.G. Lee, M.A. Belkin, R. Audet, J. MacArthur, L. Diehl, C. Pflugl, F. Capasso, D.C. Oakley, D. Chapman, A. Napoleone, D. Bour, S. Corzine, G. Hofler, J. Faist, Appl. Phys. Lett. **91**, 231 101 (2007)
21 J. Faist, M. Beck, T. Aellen, E. Gini, Appl. Phys. Lett. **78**, 147 (2001)
22 R. Maulini, PhD thesis (University of Neuchâtel, 2006)
23 B.E.A. Saleh, M.C. Teich, *Fundamentals of Photonics*, Wiley Series in Pure and Applied Optics (Wiley, New York, 1991)
24 G. Wysocki, A. Kosterev, F. Tittel, Appl. Phys. B **80**, 617 (2005)
25 G. Litfin, C.R. Pollock, R.F. Curl Jr., F.K. Tittel, J. Chem. Phys. **72**, 6602 (1980)
26 H. Ganser, W. Urban, J.M. Brown, Molec. Phys. **101**, 545 (2003)
27 H. Ganser, M. Horstjann, C.V. Suschek, P. Hering, M. Mürtz, Appl. Phys. B **78**, 513 (2004)
28 R. Lewicki, R.F. Curl, F.K. Tittel, G. Wysocki, to be published
29 A.A. Kosterev, F.K. Tittel, D.V. Serebryakov, A.L. Malinovsky, I.V. Morozov, Rev. Sci. Instrum. **76**, 043 105 (2005)